ELSEVIER

Journal of Power Sources 85 (2000) 44–48

JOURNAL OF POWER SOURCES

www.elsevier.com/locate/jpowsour

Electrochemical characteristics of Pb–Sb alloys in sulfuric acid solutions

Tokiyoshi Hirasawa [a,*], Kazuya Sasaki [a], Masami Taguchi [b], Hiroyuki Kaneko [b]

[a] *Saitama Research Laboratory, Shin-Kobe Electric Machinery Co., Ltd., Saitama, 369-0297 Japan*

[b] *Department of Materials Science and Engineering, Faculty of Engineering and Resource Science, Akita University, Akita, 010-8502 Japan*

Accepted 22 September 1999

Abstract

Lead–antimony alloys with a wide range of Sb contents, pure Pb and pure Sb were subjected to sulfuric acid solutions to elucidate their electrochemical characteristics by cyclic voltammetry and corrosion potential measurements. A corrosion test with a Pb/Sb galvanic couple was also done. For Pb-rich α-phase alloys (< 0.3 wt.% Sb), their electrochemical behavior was similar to that of pure Pb. On the other hand, for α + β phase alloys (> 0.3 wt.% Sb) their behavior was quite different from those of α-phase alloys; (i) dissolution current of Sb was proportional to Sb contents; (ii) hydrogen overvoltage was decreased remarkably with increasing the Sb contents; (iii) the corrosion potential shifted and approached that of pure Sb with time. It is confirmed that the electrochemical behavior of Pb–Sb alloys is related to the electrochemical property of the individual phase involved in the internal galvanic couples formed.

Keywords: Lead; Antimony; Lead–acid battery; Corrosion; Cyclic voltammetry

1. Introduction

Lead–antimony alloys are well known as superior grids of positive electrodes for the lead–acid battery. Many researchers have paid attention to the electrode characteristics of these alloys [1–4]. Recent researches indicate that Sb in the Pb–Sb electrode affects the microstructure and electrochemical characteristics of active materials and corrosion layers on the electrode [5,6]. Pb–Sb alloys have a merit and a demerit, one is a high performance on the charge–discharge characteristics of lead–acid battery and the other is a decrease in the hydrogen overvoltage on the negative electrode during charging. The dissolution of Sb into the electrolyte is followed by the subsequent deposit of metallic Sb on the negative electrode. The effect of Sb in Pb base metal on its electrochemical characteristics is very complex and it seems still ambiguous. One of the reasons is that only a few specimens, not a series of specimens with a wide range of Sb contents, have been studied in many cases. Furthermore, few papers discuss the electrochemical characteristics of Pb–Sb alloys in relation to the phase structure of the alloys composed of α-phase and β-phase. In this study, therefore, Pb–Sb alloys with a wide range of Sb contents were subjected to sulfuric acid solutions in order to elucidate the dependence of their compositions on their electrochemical characteristics.

2. Experimental

2.1. Specimens

Pure Pb (99.99 wt.%), pure Sb (99.9999 wt.%) and eight Pb–Sb alloys (0.005–10.14 wt.% Sb) were used. The Pb–Sb alloys are as follows: Pb-0.005 wt.% Sb, Pb-0.038 wt.% Sb, Pb-0.095 wt.% Sb, Pb-0.51 wt.% Sb, Pb-1.04 wt.% Sb, Pb-3.00 wt.% Sb, Pb-5.29 wt.% Sb and Pb-10.14 wt.% Sb. According to the phase diagram for the Pb–Sb system [7], the solubility limit of Sb in Pb is about 0.3 wt.% at room temperature. Specimens below 0.095 wt.% Sb exist as α-phase, above 0.51 wt.% Sb as α + β eutectic. Weighed Pb and Sb were melted in a graphite crucible in an electric furnace. The molten metal of 450°C was poured into an iron mold kept at 220°C in the atmosphere, to form the pieces (15 × 5 × 60 mm). Chemical compositions were determined by ICP spectroscopy (HITACHI, P-5200). Each specimen with a lead wire was imbedded in epoxy resin, with the exception of a measured area of 1.00 cm^2.

* Corresponding author.

0378-7753/00/$ - see front matter
PII: S0378-7753(99)00380-8

2.2. Corrosion test

The specimen was polished with water-resistant emery paper and buff-polished with Al_2O_3 powders. After the specimen surface had been etched in a 5 vol.% CH_3COOH, its cyclic voltammogram was measured in a 4.8 M H_2SO_4 solution at 25°C using a potentio-galvanostat (HOKUTO DENKO, HA-305). The counter and reference electrodes were a platinum mesh and Hg/Hg_2SO_4 electrode, respectively. The potential of the specimen became stable for a few minutes. The potential was scanned at a rate of 20 mV/s in the cathodic direction until −1550 mV, and then between −1550 and 1850 mV. Corrosion potential measurements were carried out with a high impedance electrometer. Furthermore, a Pb/Sb galvanic couple, in which pure Pb and pure Sb encountered each other with a separation of 10 mm and electrically connected, was subjected to the galvanic current measurement with a zero shunt ammeter (HOKUTO DENKO, HM-103).

3. Results and discussion

3.1. Cyclic voltammogram

3.1.1. Cyclic voltammogram of 10.14 wt.% Sb alloy

Fig. 1 shows the cyclic voltammograms obtained by 10 cyclic runs for a 10.14 wt.% Sb alloy. According to the literature [8], peaks (I) and (II) are assigned to the reduction of $PbSO_4$ to Pb and the oxidation of Pb to $PbSO_4$, respectively, peak (III) the reduction of PbO, and peaks (IV) and (V) the dissolution of Sb and the reduction of dissolved Sb, respectively. The current of peak (IV) was decreased rapidly after the second potential sweep. This suggests that the Sb atoms at the surface of the electrode has been almost dissolved during the first sweeping.

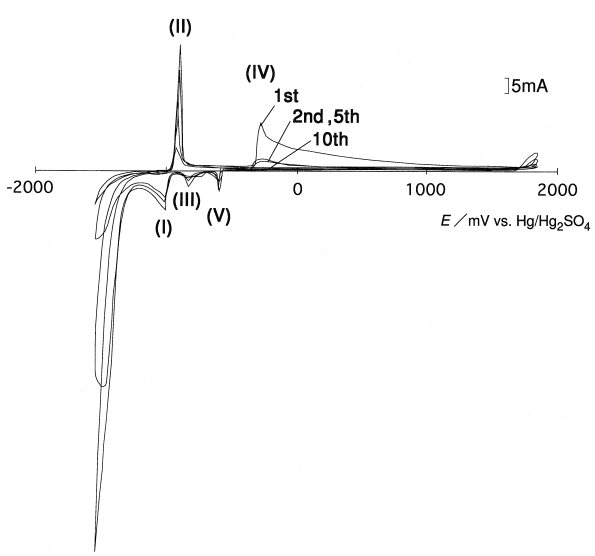

Fig. 1. Cyclic voltammogram of Pb-10.14 wt.% Sb alloy electrode.

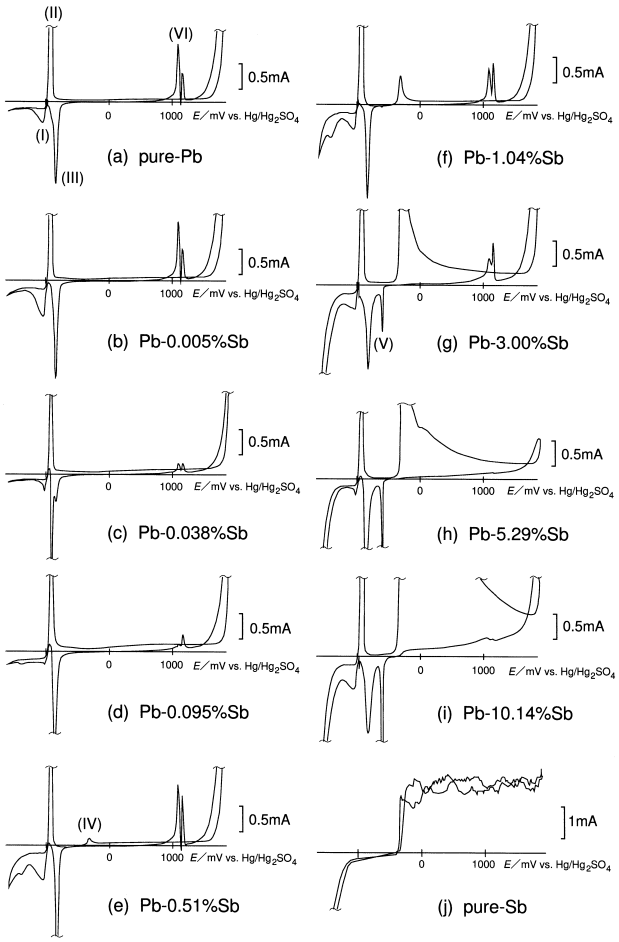

Fig. 2. Cyclic voltammograms of various Pb–Sb alloy electrodes.

Change in the cyclic voltammogram with time was further examined until 10 h after immersion. Both the hydrogen and oxygen, especially the former, generated remarkably with increasing the immersion time. A new peak showing the reduction of PbO_2 appeared in 2 h. This shows that PbO_2 grows by repeating the potential sweep.

3.1.2. Cyclic voltammograms for various Pb–Sb alloys

As shown above, the cyclic voltammogram in the first scan for a 10.14 wt.% Sb alloy shows the typical feature of the alloy itself. Fig. 2 shows cyclic voltammograms in the first scan for all specimens investigated. The curves for the Pb–Sb alloys (b), (c), and (d), which contain Sb contents of less than 0.3 wt.%, or consist of only α-phase, are similar to that for the pure Pb (a). For alloys below 0.51 wt.% Sb, a new peak or a shoulder peak appears in the cathode side of peak (III), as shown clearly for the 0.038 wt.% Sb alloy. According to Guo [9], this peak is assigned to the reduction of a basic lead sulfate.

The five cyclic voltammograms of (e), (f), (g), (h) and (i) are obtained for α + β eutectic alloys. Those profiles are different from those for α-phase alloys. A new peak (IV) appears for the 0.51 wt.% Sb alloy, and another peak

(V) appears for the alloys above 3.00 wt% Sb. Peak (V) is easily detected when peak (IV) becomes sufficiently large. It is known that the trivalent ion is stable in sulfuric acid solutions [10–12] although the pentavalent ion is expected to be thermodynamically stable. Peak (VI) almost disappears for the Pb–Sb alloys with 5.29 wt.% and 10.14 wt.% Sb. As mentioned in the previous section, however, this peak appeared for the 10.14 wt.% Sb alloy when the potential sweep was repeated. Laitinen et al. [4] showed that a 12 wt.% Sb alloy had a very small peak (VI), compared with pure Pb. Furthermore, they mentioned that the amount of product PbO_2 is decreased because the nucleation rate of PbO_2 is lowered by Sb.

The cyclic voltammogram for the pure Sb, as shown in Fig. 2(j), is different from those for the other Pb–Sb alloys. For the pure Sb, a high oxidation current passed without a special dissolution peak of Sb in the wide potential range. Laihonen et al. [3] explained that the pure Sb is partially passivated and oxygen evolution is prevented. Pavlov et al. [10–12] argued that the pure Sb is oxidized to trivalent ions and the subsequent reaction forms a gel oxide on an electrode surface, while for the Pb–Sb alloys, Sb accelerates the hydration of a PbO_2 film to repair cracks in the film during the anodic oxidation, which results in easy passivation of the electrode surface.

3.1.3. Dissolution current of Sb

The dissolution reaction of Sb occurs around −290 mV (see Fig. 2). The dissolution peak currents of Sb analyzed from the voltammograms in the first scan are shown in Fig. 3. A nearly independent line for α alloys, but a straight line with a slope of 45° for α + β eutectic alloys is obtained on log–log scale. This suggests that the Sb dissolution mechanism in the α-phase is different from that in β-phase. For the α-phase alloys, the Sb is scarcely dissolved around −290 mV. It is dispersed to the Pb matrix as the atomic size particles and internal galvanic couples formed between Pb and Sb are distributed homogeneously. For the α + β eutectic alloys, the dissolution rate of Sb is proportional to Sb content. Sb-rich β-phase is

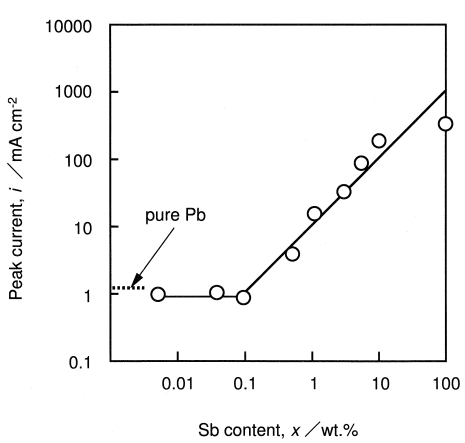

Fig. 3. Dissolution peak current of Sb at various Sb contents.

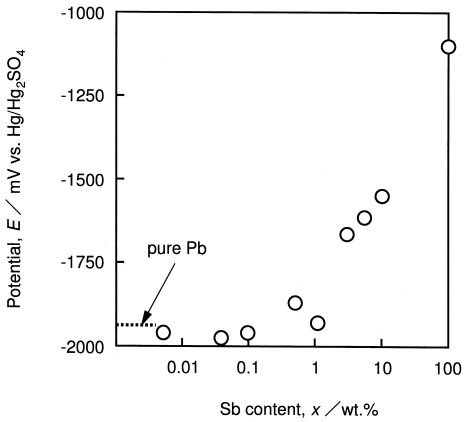

Fig. 4. Potential for hydrogen evolution at various Sb contents (potentials obtained at 3 mA cm^{-2} are shown).

dispersed heterogeneously in Pb-rich α-phase and macroscopic local cells are formed between them.

3.1.4. Hydrogen overvoltage

As a measure of hydrogen overvoltage, the potentials obtained at 3 mA/cm^2 from the voltammograms in the first scan are shown in Fig. 4. The α-phase alloy has a hydrogen overvoltage nearly the same as the pure Pb, showing that this alloy has a low activity as a catalyst for hydrogen evolution. Hydrogen overvoltage of α + β eutectic alloy is lowered with increasing the Sb contents. This shows that the α + β eutectic alloy has a higher catalytic activity. As shown in Section 3.1.1, hydrogen overvoltage was decreased with increasing the immersion time for the 10.14 wt.% Sb alloy. This shows that the dissolved Sb at the peak (IV) deposits on the electrode surface during the cathodic potential sweep, and the Sb deposit reduces the hydrogen overvoltage. Mahato and Tiedemann [13] reported that the electrochemically deposited Sb from a solution had a high activity for hydrogen evolution. Maja and Penazzi [14] pointed out that the hydrogen overvoltage of the negative electrode was lowered in a sulfuric acid solution containing 20–250 ppm Sb. The α + β eutectic alloy itself is highly active for hydrogen evolution and it is more activated due to the electrodeposition of dissolved Sb.

3.1.5. Oxygen overvoltage

As shown in Fig. 5, the potentials obtained at 3 mA/cm^2 from the voltammogram in the first scan for oxygen evolution are compared as a function of Sb contents. The potential for pure Sb is not shown in this figure, because there is no indication of the increase in the current for oxygen evolution in the range investigated (see Fig. 2j), due to the passivation of pure Sb [10–12]. Oxygen overvoltage is scarcely dependent on the Sb contents. Oxygen evolution depends on the film characteristics because it takes place on the PbO_2 film. Laitinen et al. [4] mentioned that Sb is doped into the PbO_2 film formed. Pavlov [6]

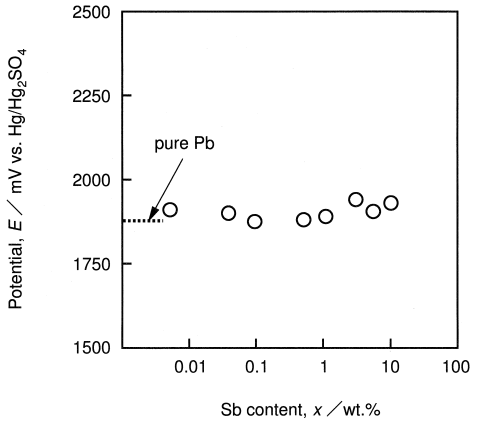

Fig. 5. Potential for oxygen evolution at various Sb contents(potentials obtained at 3 mA cm^{-2} are shown).

also reported that the amount of the hydrated PbO_2 increases with increasing the Sb contents. However, the influence of the Sb content on the oxygen evolution is not detected in this study. The reason may be that the result is obtained from the voltammograms in the first scan. It is considered that in such a short time the Sb has not been doped into the PbO_2 film sufficiently. When the potential scan was repeated for the Pb-10.14 wt.% Sb alloy, the oxygen overvoltage was lowered gradually. Therefore, it is expected that the influence of Sb contents on the oxygen overvoltage will appear with time.

3.2. Corrosion potential

Fig. 6 shows time dependence of corrosion potentials for various specimens. Immediately after immersion into the test solution, every specimen electrode except for the pure Sb had the potential of about −950 mV. The value was nearly equal to the equilibrium potential of the $Pb/PbSO_4$. For the pure Pb, the potential slightly shifted to the noble potential after 3 h. A similar behavior appeared in about 2 h for the 0.005-wt.% Sb alloy. In the case of the 0.038-wt.% Sb and 0.095-wt.% Sb alloys, the potentials suddenly shifted but returned to the nearly original value within 20 min. For alloys above 0.51 wt.% Sb, the corrosion potentials stepped up to about −380 mV in a short induction time. The potential decrease after stepping up became slower for alloys above 3.00 wt.% Sb. A temporary change in the potential for the alloys below 0.095 wt.% Sb may be due to the irregular dissolution of a slight amount of Sb from their surfaces. Moreover, the influence of the surface treatment for a specimen on the corrosion potential was observed; if the specimen was polished only by emery paper, the corrosion potential stepped up in a shorter time. Fig. 7 shows the comparison of the corrosion potentials immediately after immersion with those after 1 h. Immediately after immersion, every specimen except the pure Sb had a corrosion potential of about −940 mV, which was nearly the same as that of the pure Pb. For alloys above 0.51 wt.% Sb, however, the corrosion potential after 1 h shifted to approach that for the pure Sb. This behavior corresponds to the compositional change from α to α + β eutectic. For α + β eutectic alloys, α-phases are covered by the $PbSO_4$ formed and the covering rate is accelerated by internal galvanic couples consisting of α- and β-phases. For the α-phase alloys, internal galvanic corrosion does not proceed and their electrode potentials are kept at the equilibrium potential of $Pb/PbSO_4$.

3.3. Corrosion current and potential of a galvanic couple

Fig. 8 shows the corrosion current density and the corrosion potential for an artificial Pb/Sb galvanic couple. In this couple, the pure Pb and the pure Sb were modeled after the α-phase and the β-phase in the Pb–Sb alloy, respectively. Corrosion potentials for the pure Pb and for the pure Sb were −940 and −385 mV, respectively. A large corrosion current of about 90 $\mu A/cm^2$ passed immediately after the galvanic couple was made, and then the current was decreased steeply. Corresponding to this change in the corrosion current, the corrosion potential

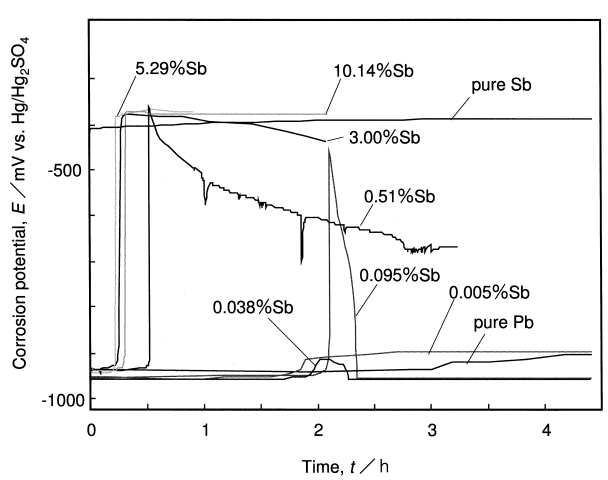

Fig. 6. Change in corrosion potential with time.

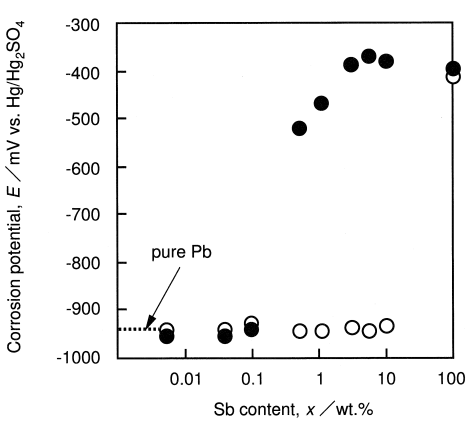

Fig. 7. Dependence of corrosion potentials on Sb contents. (○) immediately after the immersion; (●) after 1 h.

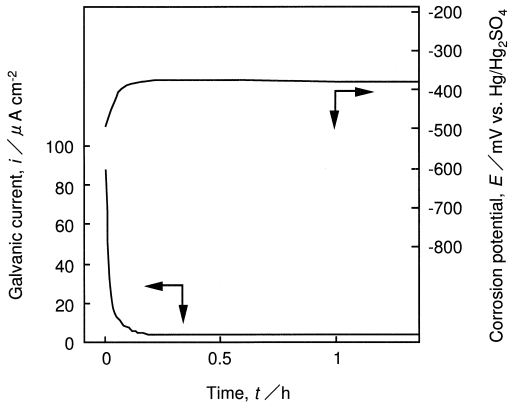

Fig. 8. Change in galvanic corrosion current and corresponding potential with time for a Pb/Sb couple.

rapidly shifted to about −380 mV which is nearly equal to the corrosion potential of the pure Sb. In the galvanic corrosion, the pure Pb acts as the anode and the pure Sb as the cathode. Each electrode reaction is known as follows:

$$\text{Cathode (Sb):}\ 1/2O_2 + 2H^+ + 2e^- \rightarrow H_2O \quad (1)$$

$$\text{Anode (Pb):}\ Pb + SO_4^{2-} \rightarrow PbSO_4 + 2e^- \quad (2)$$

$$\text{Total:}\ Pb + 1/2O_2 + H_2SO_4 \rightarrow PbSO_4 + H_2O \quad (3)$$

The reaction (2) is accelerated by the galvanic current immediately after the artificial Pb/Sb galvanic couple is completed, so that the $PbSO_4$ formed rapidly covers the surface of the pure Pb. When the pure Pb electrode is once passivated, no high anodic current is necessary to maintain the passive state. As a result, passivated Pb is easily polarized at a very low current density to reach the corrosion potential of the pure Sb. This indicates that the corrosion of the $\alpha + \beta$ eutectic alloy is governed by the existence of α-phase/β-phase galvanic couples in the alloy.

From the above results, it is concluded that the electrochemical characteristics of Pb–Sb alloys depend on whether the alloys consist of only an α-phase or $\alpha + \beta$ phases. In the case of Pb–Sb alloys consisting only of an α-phase, the dissolution current of Sb was scarcely detected. The hydrogen overvoltage was of the same level as pure Pb. The corrosion potential was around the $Pb/PbSO_4$ equilibrium potential. These results show that the electrochemical characteristics of α-phase alloys resemble that of pure Pb; that is, Sb in α-phase alloy plays no important role on its electrochemical characteristics. On the other hand, in the case of Pb–Sb alloys consisting of $\alpha + \beta$ phases, their electrochemical characteristics are distinctly different from those of α-phase alloys. The dissolution peak current was proportional to the Sb content. The hydrogen overvoltage was lowered with increasing the Sb content. The corrosion potential approached the corrosion potential of pure Sb from the equilibrium potential of $Pb/PbSO_4$. Change of the corrosion potential with time is closely related to internal galvanic corrosion formed between α and β phases.

References

[1] V. Danel, V. Plichon, Electrochim. Acta 28 (1983) 785.
[2] E. Hameenoja, T. Laitinen, G. Sundholm, A. Yli-Pentti, Electrochim. Acta 34 (1989) 233.
[3] S. Laihonen, T. Laitinen, G. Sundholm, A. Yli-Pentti, Electrochim. Acta 35 (1990) 229.
[4] T. Laitinen, K. Salmi, G. Sundholm, B. Monahov, D. Pavlov, Electrochim. Acta 36 (1991) 605.
[5] B. Manahov, D. Pavlov, J. Electrochem. Soc. 141 (1994) 2316.
[6] D. Pavlov, J. Power Sources 46 (1993) 171.
[7] M. Hansen, K. Anderko, Constitution of Binary Alloys, McGraw-Hill, New York, 1958, p. 1100.
[8] V. Danel, V. Plichon, Electrochim. Acta 28 (1983) 781.
[9] Y. Guo, Electrochim. Acta 495 (1992) 37.
[10] D. Pavlov, M. Bojinov, T. Laitinen, G. Sundholm, Electrochim. Acta 36 (1991) 2081.
[11] D. Pavlov, M. Bojinov, T. Laitinen, G. Sundholm, Electrochim. Acta 36 (1991) 2087.
[12] T. Laitinen, H. Revitzer, G. Sundholm, J.K. Vilhunen, D. Pavlov, M. Bojinov, Electrochim. Acta 36 (1991) 2093.
[13] B.K. Mahato, W.H. Tiedemann, J. Electrochem. Soc. 130 (1983) 2139.
[14] M. Maja, N. Penazzi, J. Power Sources 22 (1988) 1.